COLLECTOR ACCELERATIONS PROCESSING FOR CONDITION-BASED MONITORING OF OVERHEAD LINES

Marco CARNEVALE, Andrea COLLINA

Dipartimento di Meccanica, Politecnico di Milano
Via La Masa 1, 20156 Milano, Italy
e-mail marco.carnevale@polimi.it
ph. +39 02 2399 8437 fax +39 02 2399 8492

Post-print version

To cite this paper:

Carnevale, M., Collina, A.
Processing of collector acceleration data for condition-based monitoring of overhead lines (2016) Proceedings of the Institution of Mechanical Engineers, Part F: Journal of Rail and Rapid Transit, 230 (2), pp. 472-485. DOI: 10.1177/0954409714545637

Published version: https://journals.sagepub.com/doi/10.1177/0954409714545637

ABSTRACT

This paper describes a diagnostic system for overhead line monitoring, based on the measurement of collector accelerations. It is aimed at marking an improvement on current scheduled methods for catenary and pantograph maintenance, making condition-based maintenance possible. The set-up proposed is inexpensive and easy to install on commercial service trains. Meaningful indications on pantograph-catenary interaction are obtained by the processing and analysis of collector accelerations; summarised values are computed in real time during the train run and compared with alarm limits.

Keywords: pantograph, catenary, condition based monitoring, real-time diagnostic.

1. INTRODUCTION

The operation of a high-speed line requires a high level of performance and reliability from both the overhead line and the pantograph. For this reason, to keep the status of the infrastructure under proper control, the overhead contact lines (OCL) of all major railway networks are periodically monitored using inspection vehicles that measure geometrical parameters of the contact wire such as height, stagger and also, in some cases, thickness. The output of this procedure is the geometrical condition of the OCL, and this is compared with levels usually laid down by national or international standards.

At a second level, instrumented pantographs on dedicated inspection trains permit direct monitoring of pantograph-catenary interaction at commercial or lower speeds (examples are Archimede, IRIS train [1], DR Yellow). In this way the effect of OCL status on current collection quality can be measured and again compared with national standards and with Technical Specification for Interoperability (TSI) requirements, as far as contact force peak values and standard deviation are concerned. These infrastructure inspections can only be performed at rather long intervals, because they are carried out by a single train that has to cover the whole network, or because they can be performed only when regular service is interrupted (e.g. at night during the four-five traffic free central hours) [2].

Both of these inspection methods can monitor the state of the OCL in the long term, giving indications for standard periodic maintenance operations, but cannot monitor short-term degradation or defects that are likely to cause disruption of regular service. In other words, they

are not able to prevent the occurrence of accidents, and so do not strictly contribute to increasing the safety level of regular operations.
In order to get a more detailed picture of both pantograph and catenary state at commercial speed, and thus achieve continuous infrastructure monitoring, it would be necessary to fit some or, when necessary, even all trains in an entire fleet with a monitoring system. This system, combined with interpretative modelling, would not only permit detection of hot-spots and keep an eye on them before they degenerated into faults, halted trains and accidents, but would also provide a diagnosis of OCL status, so that suitable maintenance operations could be programmed. The essence of a diagnostic system is the comparison of significant measured quantities against a reference condition, depending on operational parameters such as train speed or pantograph preload. The analysis of relevant indices obtained from data processing would permit diagnosis of the possible cause of the malfunction, while the trend of the index would indicate the rate of deterioration of the defects found. For the case of pantograph-catenary interaction, a diagnostic system should include the following items:

- a measuring system that must be non-intrusive, easy to maintain and affordable, giving robust signals that would then be processed;
- a device for locating the train's position along the line, in order to assign to a given defect its exact position;
- an on-board unit able to process the signals measured in order to reduce the amount of data to be transmitted to ground, providing an efficient and significant summary through the calculation of suitable indices;
- a data transfer system from the on-board device to a ground station where a trend analysis would be performed for each line or for particular sections.

It is worth recalling once again that it is mandatory to have a comparison level for all the indices considered, so that their variation can be used for diagnostic purposes with respect to a reference data base. Such diagnostic activity, as summarised above, is complementary to normal inspection activity and is aimed at preventing the effects of short-term failure or defects, permitting follow-up on a daily basis and thus increasing the safety level of train operation. This can obviously have a positive impact on maintenance strategy too, permitting optimisation of maintenance operations alongside regularly programmed maintenance.
The advisability of improving present-day scheduled monitoring and maintenance by using diagnostic systems installed on commercial service trains has been pointed out in several articles [3,4,5,6,7] as a way of providing a constant flow of information on overhead line status, improving prevention of failures and service interruptions, and paving the way towards condition-based maintenance. Since current collection quality mainly depends on contact force variability, this is commonly considered the best parameter for assessing pantograph-catenary interaction. Different solutions have been proposed, based on measurement of the contact force [3,4], or on its estimation by pantograph state, e.g. in an Extended Kalman Filter [5]. This latter technique overcomes the need for reliable contact force measurement, which is no small advantage. The importance of developing a low-cost device, and therefore the need to simplify the measurement set-up, was also pointed out in [6], where the problem of decoupling high voltage cables at their crossing from the pantograph to the car-body roof is overcome by measuring pantograph head (pan-head) motion with infrared non-contact measurements. In [7] accelerometers are installed in vicinity of the carbon strip, and a Digital Processing Module directly clamped on the 25 kV pantograph structure transmits information via Bluetooth to a Signal and Relay Unit installed inside the carriage.
This paper describes a rolling stock based monitoring system [2] mainly aimed at infrastructure diagnosis, with possible implications also for pantograph anomaly identification. The main idea is to use pan-head accelerations to identify the behaviour of contact force, so as to develop a

non-intrusive low-maintenance measurement set-up that can be installed on an ordinary fleet of trains (e.g. a high speed train fleet) and that is able to recognize relevant defects. The lowest possible number of sensors is used to contain costs of the instrumented pantograph. In the application proposed one optical accelerometer is mounted on each of the two collectors, and each sensor is connected by optical fibre to the acquisition and processing unit in the car-body, without any need to power the sensors. This solution is much simpler than the standard set-up used for the measurement of contact force, which requires a greater number of sensors (See European Standard EN50317). It is also easier to set, since the ability of optical fibres to electrically insulate the sensor from the conditioning and data-acquisition unit permits very straightforward wiring [8,9,10]. Moreover, the use of accelerometers allows measurement to be extended to a larger frequency band, allowing more information to be collected.

The measurement of pan-head acceleration can be used satisfactorily for diagnostic purposes since the contact force, and therefore current collection quality, is directly related to pantograph acceleration. Inertial terms are in fact the main component of contact force in the frequency range related to dropper periodicity, and also have a significant role at span-passing frequency [4,11]. Moreover, it has been demonstrated [12] that high frequency vibrations related to collector flexural normal modes have a significant role in the generation of contact losses: these contact force components are not yet measured in standard applications [8,9,10], nevertheless the extension of the measured acceleration up to 200 Hz allows useful information to be obtained on the level of excitation of the flexural modes, and therefore on current collection quality [13]. In such a way a broad range of frequencies potentially excitable by several line defects can be detected.

In the following sections a description of the diagnostic and geo-localization systems is given, together with the data processing techniques developed for diagnostic purposes. Two levels of analysis are performed: on-board analysis, aimed at the real time identification of local and distributed catenary defects and pantograph faults. Remote analysis, consisting in the long-term comparison of the data acquired, which would identify a trend for infrastructure and pantograph status so as to detect longer-term incipient faults. (not dealt with in this paper).

The diagnostic system was installed on the ETR500-Y1 train equipped with an ATR95-25kV pantograph, which is used as inspection train. The pantograph adopted for the experiment was therefore already fitted with a standard set-up for contact force measurement, used as a reference to define how to analyse the acceleration raw signals and develop correct algorithms for identifying defects. Application to the first data collected is presented.

The paper is organized as follows:

i. analysis of the relationship between contact force and pan-head acceleration.
ii. Description of the optical measurement set-up proposed for the diagnostic system (to be installed on commercial trains) and description of the traditional set-up for contact force and displacement measurement (to be used as reference in the validation of the methods proposed).
iii. Data processing for overhead-line (OHL) local defects detection.
iv. Data processing for OHL distributed defects detection.
v. Concluding remarks.

2. THEORETICAL BASIS: RELEVANCE OF PAN-HEAD ACCELERATIONS

The analysis of pantograph-catenary dynamic interaction, aimed at evaluating current collection quality, is normally performed in the 0-20 Hz frequency range as prescribed by the EN50317 specification. Limits are set in international and national standards for extreme values of contact

force, aimed at preventing excessive uplift and mechanical wear or contact loss and electrically related wear. All the phenomena related to span and dropper periodicity occur in this frequency range, and a well-established method for contact force measurement is adopted worldwide. In detail, the excitation due to span periodicity falls in the 0.5-2 Hz frequency range (e.g. 1.46 Hz for a 57 m span length at 300 km/h), the excitation due to dropper periodicity falls in a broader and higher range (8-14 Hz for the instance of dropper spacing from 6 to 10 m at 300 km/h). Moreover, the first two natural frequencies of the pantograph, which most relevantly affect its dynamics, fall within the frequency range 0-8 Hz for all the high-speed pantographs in operation today. These frequencies are related to the two modes of vibration characterized by the articulated frame and the pan-head vibrating in phase and out of phase respectively. Figure 1 shows the experimental frequency response functions (FRF) of pantograph head acceleration for a unit contact force, obtained by laboratory tests (modulus in Figure 1a and phase in Figure 1b). Several high-speed pantograph results are reported, here named as type A, type B and type C. For each pantograph, the first and the second modes of vibration are visible (phase equal to -90 degrees), respectively in the frequency ranges 0.4-0.8 Hz and 4-7 Hz.

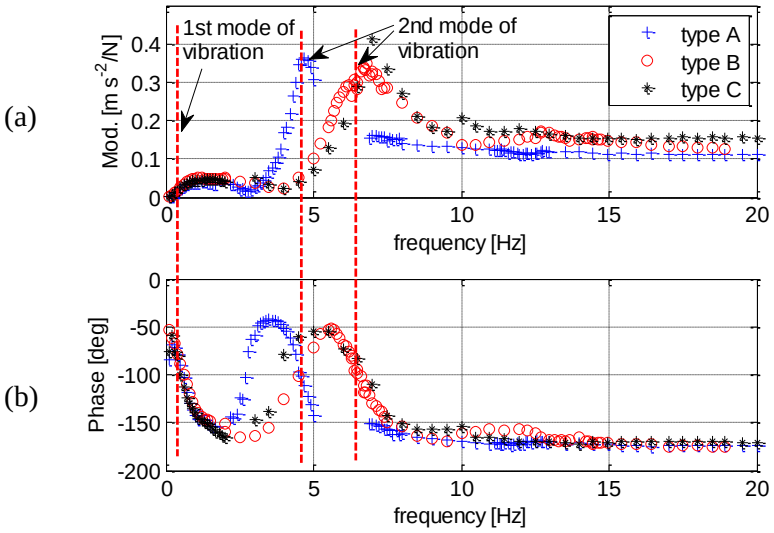

Figure 1: Experimental frequency response functions of three high speed pantographs. Pan-head acceleration for a unit contact force. (a) Modulus. (b) Phase.

In the analysis of pantograph dynamics it is worth recalling the link existing between the contact force and pantograph accelerations. The modulus of the FRF reported in Figure 1a tends to a constant value for frequencies higher than the second mode of vibration, i.e. the one with pan-head and articulated frame in phase opposition. In this frequency range (seismic zone) the pantograph response is dominated by inertial forces, as demonstrated by the reciprocal of the reported modulus (i.e. contact force over pan-head acceleration): for all the pantographs considered the ratio between the force applied to the collector and collector acceleration is close to the pan-head mass. During operation the pantograph is excited in this frequency range by dropper passing frequency, so that it can be assumed that pan-head accelerations are good indicators of pantograph contact force as far as the frequencies related to dropper passing are concerned.

The accelerations measured on pantograph collectors can give significant information on contact force variability also in the case of span-passing frequency. This frequency, in the case of high-speed trains (e.g. 1.46 Hz for a 57 m span length at 300 km/h), is usually higher than the first mode of vibration of the pantograph (see Figure 1). Figure 2a shows the total contact force obtained by numerical simulation [14] with an ATR95-25kV pantograph running at 300

km/h along the Italian C270 catenary, computed as the sum of the contact forces F1 and F2 acting on each single collector. In the spectrum at the top of the Figure **2**a, the total contact force component corresponding to the span-passing frequency is highlighted. This force component is represented, in terms of amplitude and phase, by the arrow in the polar diagram of Figure 2b (circle marker), the reference assumed for phase computation being the mast position. The additional markers in the polar diagram represent all the pantograph forces balancing the total contact force at the same span-passing frequency, which are in particular articulated frame inertia (hexagram), pan-head inertia (star), air spring and damper forces (diamond and square respectively), as indicated in the scheme of the pantograph model in the same figure. In the model, the degree of freedom relative to the articulated frame is reduced to the point of connection to the head suspension, so that the spring and damper forces acting at the base of the frame are also reduced to the same point. It can be noted that the main force generating the total contact force is the articulated frame inertia, which is practically in phase with the pan-head inertia, the first mode of vibration being still dominant at the frequency considered. Therefore, the measurement of pan-head acceleration can be assumed as an indicator of contact force amplitude [4]. The value of the articulated frame inertia is twice the pan-head inertia both because of its greater mass, and because of a greater level of acceleration (pan-head acceleration at span frequency is around 30% lower than frame acceleration in the case considered.)

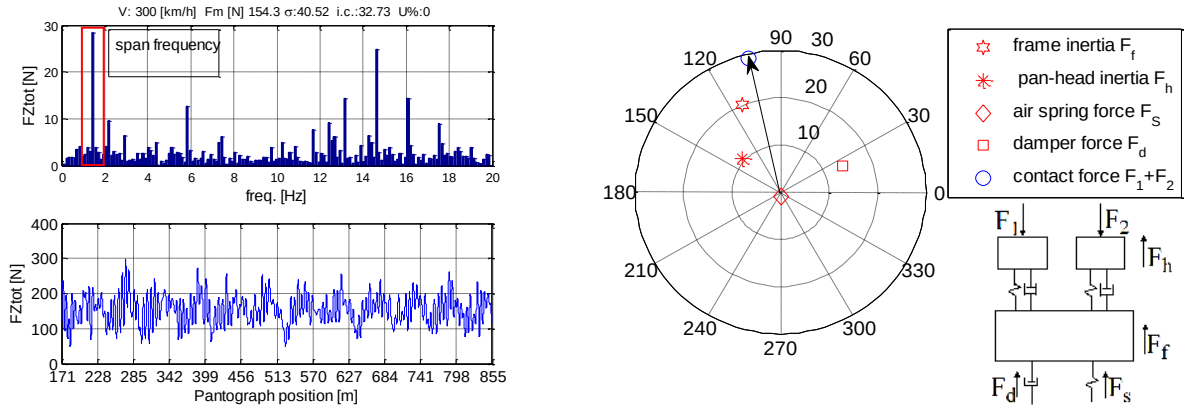

(a) (b)

Figure 2 : Span-passing frequency contact force analysis: (a) Numerical contact force results. (b) Polar diagram of span-passing frequency pantograph forces.

After describing the relationship between pantograph accelerations and contact force in the case of span and dropper related frequencies, attention is now drawn to rather higher frequencies. In [12] it was demonstrated that high frequency vibrations related to collector flexural normal modes play a significant role in the generation of contact losses. These frequencies can vary for different shapes of the collectors, but, as pointed out in [12], they still remain in a well defined frequency range for different pantograph types (starting from 50 Hz). High frequency vibrations are in particular excited by contact wire irregularity and impacts due to singularities in contact wire lay-out, so that the extension of contact force measurement up to a frequency of 200 Hz would be a helpful instrument for improving the evaluation of current collection quality. The present method of contact force evaluation is suitable up to a frequency of 20 Hz (EN50317): in this range the collector acts as a rigid body, so that the two accelerations measured for each collector can be used to calculate its inertia force. This force can then be added to the one directly measured by load cells at each collector support, so as to obtain the total contact force. A preliminary study regarding the possibility of extending the contact force measurement range up to 200 Hz was pointed out in [10]. In current applications, even if contact force components

related to collector flexural vibrations cannot yet be measured, the extension of the acceleration measured up to 200 Hz permits the acquisition of useful information on the level of excitation of these flexural modes, and therefore on the defects mentioned above. Figure 3 shows an example of acceleration power spectral density, corresponding to a 300 km/h test run, in which it is clearly visible that collector flexural modes are excited both on the front and rear collectors. The level of excitation on the leading collector is significantly higher than that on the trailing collector. The first mode at 63 Hz is hardly visible on the leading collector, and not visible at all on the trailing collector, since the two accelerometers are placed close to the nodes of the modal shape.

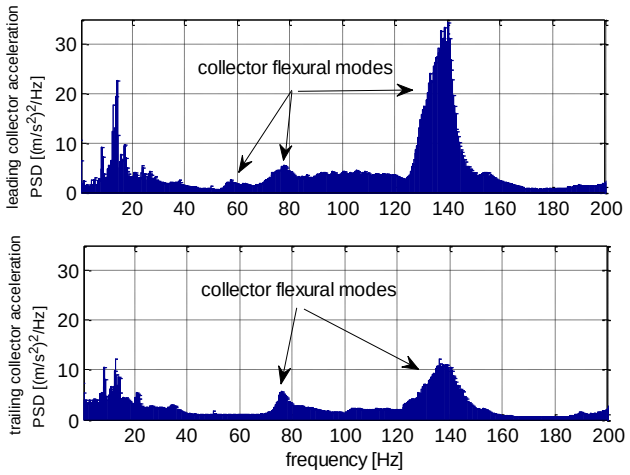

Figure 3: Measured acceleration power spectral density. (a) Leading and (b) Trailing collector.

3. MEASUREMENT SET-UP

The diagnostic system components were installed on the ETR500-Y1 test train, a special train for experimental and test purposes. The sensors were placed on an ATR95-25 kV pantograph. The aim of the campaign was to try out a prototype multi-purpose condition-based monitoring (CBM) system designed to be as similar as possible to a feasible product for service high-speed trains. For this reason reliability, autonomous operation, integration with on-board train equipment and remote communication were taken into account as important features.
Pan-head acceleration measurement is performed by means of optical accelerometers based on the principle of light intensity modulation, which has the advantages of not requiring local power and not needing a highly expensive frequency demodulator as do Fibre Bragg Grating (FBG)-based sensors. The accelerometers were customized, in cooperation with the manufacturer, so as to be suitable for pantograph application. Particular effort was put into getting the best trade-off between high resolution and a resonance frequency sufficiently high and damped so as not to be excited during operation. Table 1 summarises the sensor's main characteristics.

Sensitivity	Natural frequency	Frequency range	Full scale
10 mV/(m/s^2)	700-800 Hz	1÷300 Hz	50 g

Table 1: Optical accelerometer main characteristics.

The ATR95-25kV pantograph adopted for the experiment has two independent collectors, and it is therefore desirable to use at least one accelerometer per collector. Collector roll motion is not possible in the particular suspension, as it is prevented by a torsion bar. Nevertheless, front

and rear collector accelerometers are placed in a crossed configuration as in Figure 4a, so as to record differences in right-side and left-side motion generated by flexure-torsional pantograph modes and contact point position lateral displacement due to stagger. Figure 4b shows a detail of an installed sensor: particular care was taken to guarantee a minimum curve radius of the optical fibre greater than 50 mm, and to avoid optical fibre flexural movements during operation. In addition, the sensor's position was chosen so as not to interfere with periodical strip substitution operations.

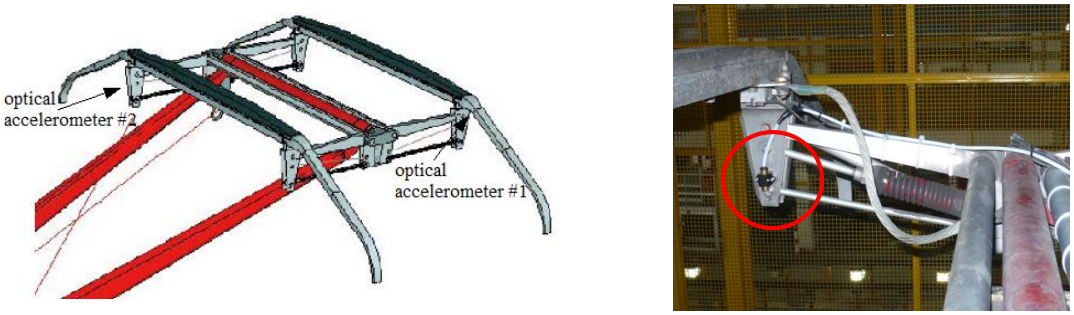

(a) (b)

Figure 4: Optical accelerometers layout. (a) Positioning on the two collectors. (b) Sensor positioning detail.

The use of optical sensors permits very straightforward wiring, owing to the intrinsic insulating properties of optical fibres. The sensors are directly linked from the high voltage pantograph to an electronic board placed inside the car-body, without the need for additional insulating devices. The board high-pass filters the signal with cut off frequency 0.5 Hz and converts it into an analogue ±10V signal. This signal goes through an anti-aliasing filter and is then sampled at a sampling rate of 500 Hz and 16 bit resolution by an acquisition and processing board. Acceleration data are real-time processed during the train run using dedicated algorithms. As will be explained below, summary indices are computed and compared with alarm limits so as to detect any defects.

The architecture of the overall system is based on an ethernet network connecting the pre-existing train data network to the CBM boards, dedicated to data acquisition and processing, and to a GPRS communication system, used to transmit the data to a ground device. The algorithms implemented in the real-time processing board use data retrieved from the vehicle logic such as speed, line and signalling balises ID, operating pantograph and master loco. All the devices connected via the Ethernet network have synchronous clocks, so that delays in data transmission can be monitored.

The train's position is identified by the signalling balises, whose ID is detected during the run. Train localization using classical phonic wheels is in fact not reliable enough for diagnostic purposes, since it is subjected to drifts, especially those accumulated in curves [2]. The position of each balise, stored in a database, is therefore used to correct continuously the train position obtained by a phonic wheel. Since the distance between two consecutive balises is around 1 km, the position of the defects can be accurately identified, thus facilitating maintenance operations.

The on-board processing of raw signals allows the amount of data to be reduced, and only diagnostic indicators are transmitted via GPRS, together with current speed, pantograph operating condition and actual position, to a ground server where they are collected and post-processed for an off-line trend analysis. Two levels of analysis are thus performed: on-board analysis aims at real time identification of local and distributed catenary defects and pantograph

fault, while remote analysis (not dealt with in this paper) consists in the long-term comparison of the data, as to define a trend for the infrastructure and pantograph status.
The same pantograph fitted with the optical sensors for diagnostic purposes, designed to work with only two sensors in the case of commercial trains, was equipped in this study also with a standard set-up for contact force and contact point displacement measurement, normally used for certification of the infrastructure according to EN50317 specifications. The pre-existing measurement set-up is therefore in parallel with the optical measurement system, so that the proposed diagnostic techniques can be validated by relating the alarms obtained from accelerometer analysis with measured contact force and contact point and frame vertical displacement.

4. DETECTION OF OVERHEAD LINE LOCAL DEFECTS

As far as experience on the Italian high-speed network is concerned, the two main sources of OHL local defects are midpoint anchor misregulation and incorrect overlaps positioning, also shown in detail in [4]. These defects result in contact force peaks and in the excitation of pantograph and collector flexural modes, with a consequent increase in the power of the acceleration measured [15]. Experience gained during many test runs showed in particular that the cause of the highest contact force peaks is related to misregulation of the midpoint anchor. Figure 5a represents the scheme of the type installed on the high speed catenary C270 in the centre of each tension length (around 1 km). The contact wire and its suspension hangers can move only within the constraints highlighted in the Figure 5b. When the pantograph approaches the constraint, the pin slides into the guide so that a certain contact wire uplift generated by the pantograph force is permitted. This movement can be blocked when misalignment between pin and guide causes friction, or when the pin is installed by mistake at the end of its stroke, as in the picture in Figure 5b showing a lab set-up.

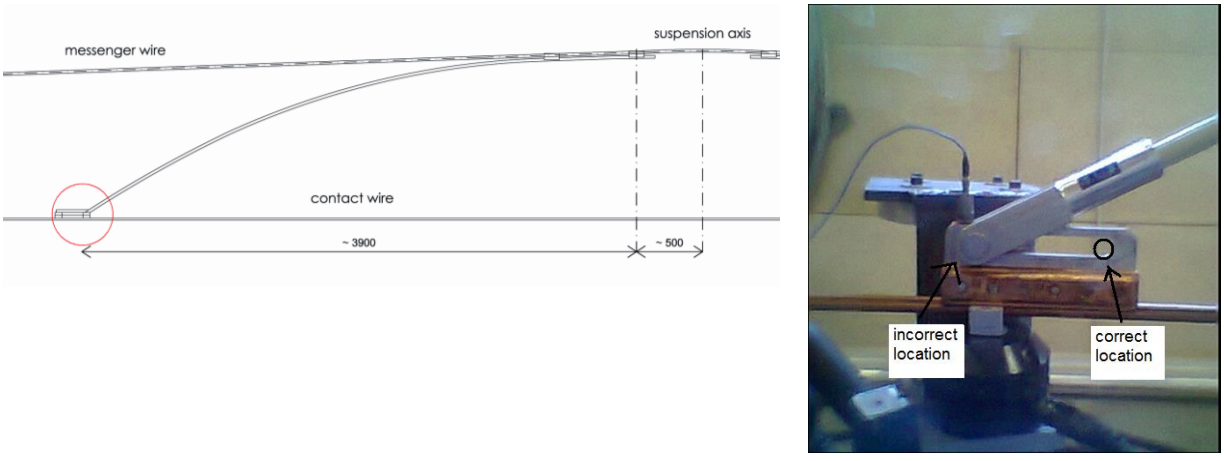

(a) (b)

Figure 5: Midpoint anchor of the Italian high speed catenary C270. (a) Scheme. (b) Detail of the faulty regulation with end of stroke pin.

In these cases significant contact force peaks can occur. In order to illustrate this effect, Figure 6 shows the experimental contact force measured with the reference set-up (EN50317) during track tests, for a length corresponding to two catenary sections (speed 300 km/h). From top to bottom, total contact force, front and rear collector contact forces and stagger are reported. Force signals are low-pass filtered with a 20 Hz cut-off frequency. Each tension length is identifiable by stagger: since the section is on straight track, the stagger signal is close to a

triangular wave, interrupted (km 70.65, km 69.6 and km 68.6) when the pantograph enters the incoming contact wire under the overlapping section, and the contact point location on the collector changes abruptly. In the middle of each tension length at km 70.1 and km 69.1, where faulty midpoint anchors are installed, the total contact force (upper figure) exceeds the European Technical Specification for Interoperability (T.S.I.) limit of 350 N. When considering the contact forces concerning each collector, it can be noted that the highest peaks (258 N) are measured on the front collector F2, whereas on the rear collector conditions close to contact loss can be detected. This is because the front collector is the first to make contact with the blocked constraint, and is in agreement with the general trend observed for leading collector contact force variability, which is always higher than that related to the trailing collector (e.g. the contact force standard deviation in the analysed case are σ_{F2}= 24.2 N for the front collector, σ_{F1}=20.9 N for the rear collector).
In Figure 6 another contact force peak approaching the T.S.I. limit is visible at km 69.6, at the location of section overlap. As described in [4] this is likely to be another critical local defect, where high contact force occurs.

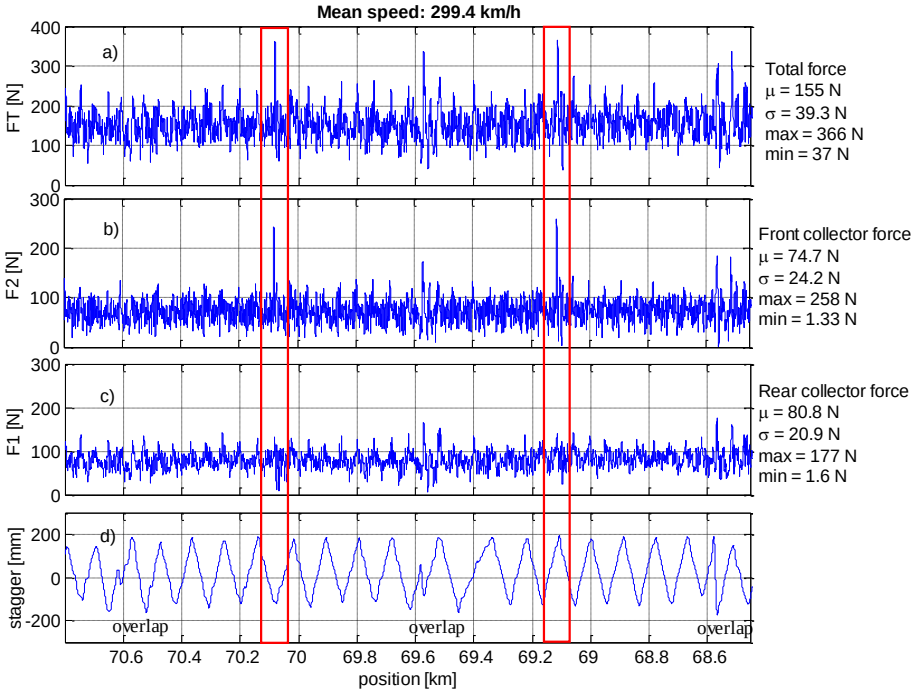

Figure 6: Contact forces peaks at the locations of faulty midpoint anchors (km 70.1 and km 69.1)

The same catenary length is now analysed to examine how to process acceleration signals in order to extract a proper defect signature. Figure 7a shows the accelerations measured by the optical sensors on the front and rear collectors, corresponding respectively to the contact forces F2 and F1 of Figure 6. At the location of the two faulty midpoint anchors (km 70.1 and 69.1), a high acceleration level is visible, but maximum and minimum peaks of the row signals can hardly be used to identify unequivocally local defects. In fact they do not differ enough from the acceleration background, and can be confused with other acceleration peaks if defect detection is carried out merely by identifying a simple threshold overshoot. Moreover, the raw signals can show spikes that do not in fact correspond to a line defect. In order to overcome this aspect, proper data analysis is performed, aimed at highlighting the power increase of the accelerations at the location of local defects. The root mean square value (RMS) of both collector accelerations (frequency content 0.5-250 Hz) is calculated over a mobile window of

short length and a high level of overlap, directly by using the time samples. The main idea behind this technique is to distinguish the power associated with the acceleration peaks, so as to distinguish occasional peaks from those generated by a real defect. Figure 7b shows as an example the results obtained by RMS analysis with T=0.2 s and a 90% overlap, and proves that acceleration signals can be used to identify the malfunctioning of singular points: peak values in RMS of front and rear collectors can be detected at the locations of the two midpoint anchors, corresponding to the contact force peaks of Figure 6. Real acceleration peaks are distinguished from spikes: since the spike's duration is much lower than the time window T=0.2 s, it is filtered by the RMS computation. A peak is detected simultaneously both for front and rear collectors: even if front and rear collector accelerations present a time shift due to the distance between the two collectors (0.008 s at 300 km/h), the time window used for the analysis is long enough to get the A1 and A2 RMS maximum peaks at the same location, and to unequivocally identify the local defect. Therefore, analysis of the mobile RMS of the sum of the two signals can be used to strengthen the identification of a local defect, and to take into account the possibility that, owing to stagger, the two collectors are excited with differing intensity.
In regular spans with no local defects, an average RMS variability associated with span periodicity is present, owing to the non-constant mechanical impedance along each span. Local defects can be detected simply by a level comparison, which is very suitable for real time application: RMS alarm thresholds can be set based on the corresponding measurements of contact force peaks, stored in a data base easily compilable during the phase of pantograph certification, when the contact force has to be measured according to EN50317.

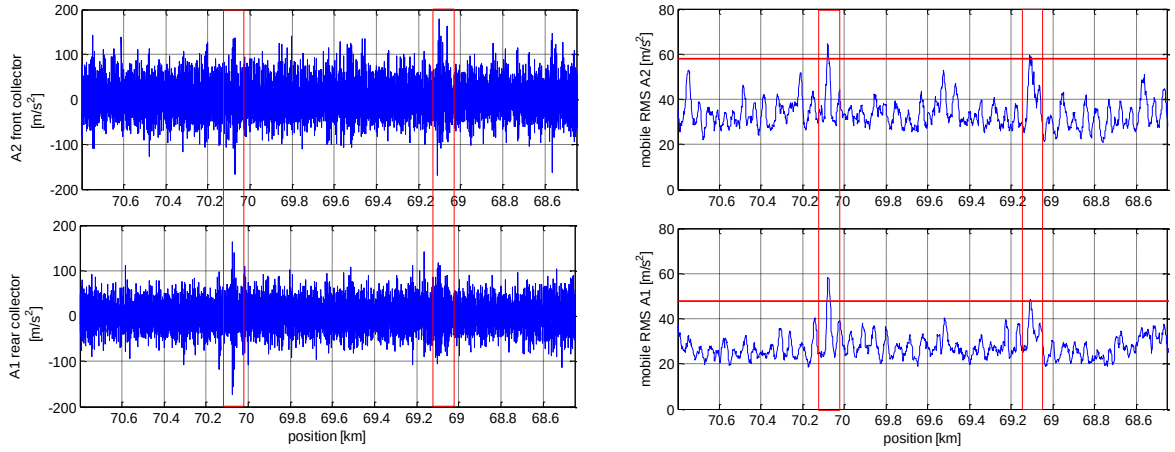

(a) (b)

Figure 7: Acceleration of front and rear collector. (a) Raw signals. (b) Mobile RMS computed over a short window T=0.2 s, overlaps 90%.

The optimal time window length *T* has to be set according to two targets: the capability of RMS analysis to clearly identify local defects, quantifiable by the comparing peak value amplitudes with RMS average variability in a standard catenary length, and the computational effort demanded of the real time board processing the data. Some considerations can be made by analysing the duration of the decay excited by the impact with the local defect: Figure 8 shows an enlarged view of the acceleration signals corresponding to the position of the local defect at km 70.1. An increase in the acceleration level, lasting approximately 0.2 s, is visible both on front and rear collectors, and a time shift between the two acceleration signals is visible owing to the distance between collectors. This behaviour is observed in most local defects detected during experimentation, so that the time T=0.2 s can be assumed as distinctive of the defect taken into account.

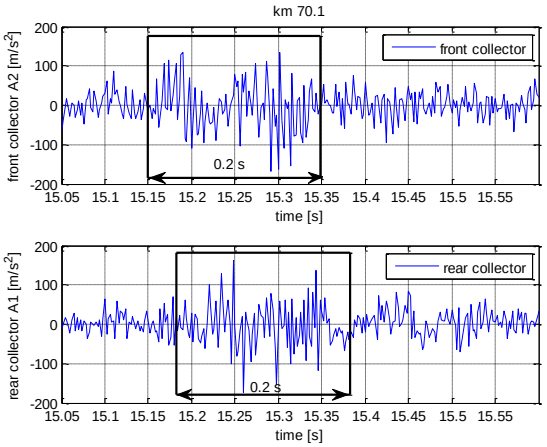

Figure 8: Enlarged view of the acceleration signals corresponding to the defect at km 70.1. (a) Front collector acceleration. (b) Rear collector acceleration.

The duration T is mainly related to the dynamic response of the pantograph to the OHL local defect. The dependence on train speed is mostly affected by the fact that, for a given defect, an higher level of vibration is excited at higher speeds, and therefore a longer response is observed. Moreover, it is important to remark that the time T may also depend on the pantograph, as pantograph with different collector mass or damping could react with different response time. For a given pantograph and speed range, it can be assumed that a time window larger than the common decay duration (i.e. T=0.2 s for the case considered here) reduces the RMS peak values, since it averages both signal portions with anomalous and standard acceleration levels and smoothes out irregularities. On the other hand, a larger time window T reduces the variability of the RMS signal within regular spans, making the RMS peaks more identifiable with respect to the background level. The best compromise can be found using the *crest factor*, computed on the RMS signal as the ratio between the RMS peak value at the location of local defects and the standard deviation of the overall RMS signal: a high level of the *crest factor C* gives an easy reading of the peaks associated with local defects.

$$C = \frac{RMS_{peak}}{RMS_{st.dev.}}$$

Figure 9 shows the crest factor values corresponding to the faulty midpoint anchor at km 70.1, as a function of the time window length T. Time windows equal to 0.05 s, 0.1s, 0.2 s. 0.3 s and 0.4 s are considered. The crest factor value relative to the front collector (Figure 9a) shows a monotonic decrease and a significant change of slope for a time window longer than T=0.2 s, whereas the rear collector data (Figure 9b) present a maximum in T=0.1 s. Based on these results, T=0.2 s can be assumed as the upper limit, while the lower limit is selected by taking into account the computational effort demanded of the real time board computing the RMS value during the train run: the shorter the time window, the higher the number of operations per second required.

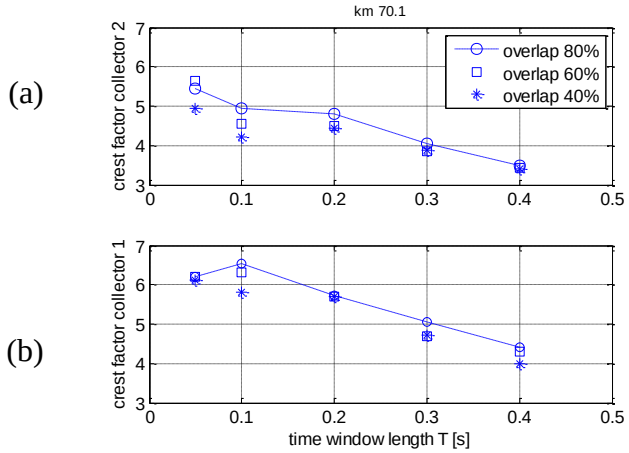

Figure 9: Crest factor for varying time window lengths T and window overlap. Local defect at km 70.1 (a) Front collector. (b) Rear collector.

The computational effort is also the guideline for the choice of window overlap: a large overlap avoids the power content associated with a defect being split into different windows, and so has beneficial effects on the RMS peak amplitudes and also on the crest factor. On the other hand, the percentage of overlap has to be limited in order to reduce the number of operations required. The crest factor results corresponding to window overlaps equal to 80%, 60% and 40%, calculated for each of the considered window lengths T, are shown in Figure 9: the reduction of window overlap from 80% to 40 % reduces the crest factor value by approximately 15% in the worst case (T=0.1s).

4.1 Data repeatability

Repeatability of the calculated data is essential for developing a reliable condition-based maintenance system. For this reason, the data obtained in different train runs were compared to verify the persistence of the main RMS peaks at the same positions. The results from four out of seven train runs performed along the same section length within a week are shown in Figure 10. No maintenance was carried out during the test session. From top to bottom, the measured contact force (Figure 10a), front and rear acceleration RMS (Figure 10b and Figure 10c respectively) and the RMS of the summed signals (Figure 10d) are shown.

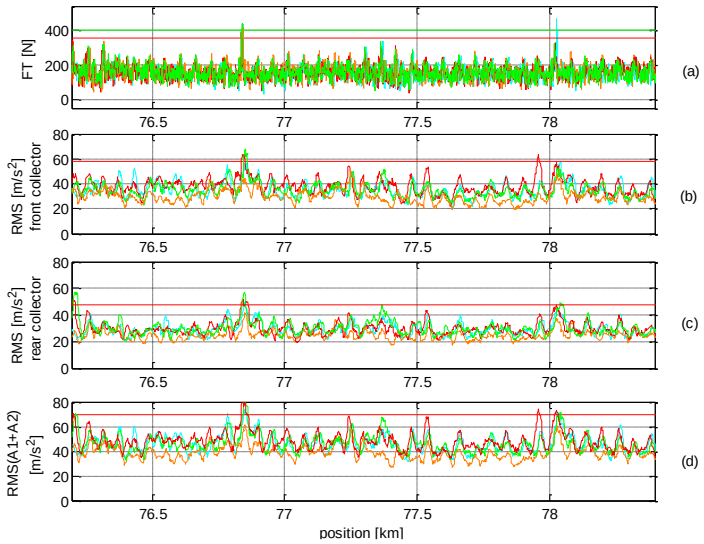

Figure 10: repeatability of the mobile RMS computed on the acceleration signal with frequency content 0-250 Hz.

A first remarkable result is that good repeatability is obtained both in contact force and RMS values, with the main contact force peaks clearly highlighted by acceleration RMS in the majority of the test runs. Moreover, the average value of the RMS of front and rear collector acceleration is similar regardless of the test line, with the leading collector RMS mean value higher than that of the trailing collector. This is made clear by comparing the results of Figure 10b and Figure 10c, relating to tests performed along one line, with the results of Figure 7b, referring to another line which is nominally equipped with the same catenary.
A certain level of variability is observed both in the measurements of the contact force and in acceleration RMS carried out in several test repetitions, due to the fact that the state of the line is not exactly the same at each pantograph passage (e.g. the contact wire position at the steady arm location can change due to the friction related hysteresis, dropper inclination can arise due to differential thermal expansion between contact wire and messenger wire in different days). The aim of the comparison among several passages is also to reinforce the detection of permanent defects. In Figure **10** each test repetition detects an RMS peak in correspondence with the two contact force maxima, but the absolute values of the contact force and RMS peaks can in some cases show a significant difference between subsequent tests; moreover, an important RMS peak is detected at km 77.9 in only one of the tests and is not confirmed by other test run results.
Figure 11 shows, as a function of train position along the track, the number of occurrences of contact force peaks exceeding 350 N, recorded during all the seven run tests repeated along the same track (total length 50 km). Contact force peaks occur with significant repeatability at specific locations, showing some singularities in the quality of pantograph-catenary interaction. Nevertheless, only in seven points out of twenty is the repeatability higher than 50%. In all the other cases, contact force peaks exceeding 350N are measured for less than half the sample.

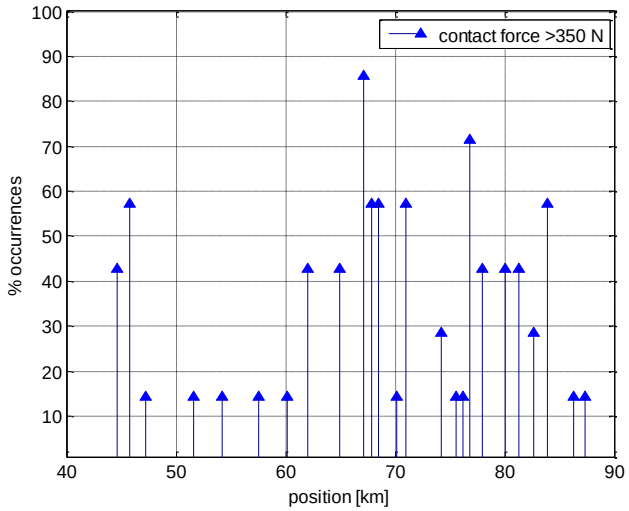

Figure 11: Number of occurrences of contact force peaks exceeding 350 N. Series of seven test runs.

The monitoring method proposed is based on the collection of a large quantity of data available from the train fleet. The acceleration RMS measurements from several commercial trains will be therefore available to help identify the line hot-spots, which can be identified as the points where a high number of RMS occurrences exceeding the threshold are found. In order to analyse comparable data, with contact force and acceleration not significantly affected by the actual speed [15], different thresholds corresponding to different speed ranges have to be set. The experimental data available are treated in this paper in a similar way to those in the final application: only the points where the contact force (only available at the experimental stage)

or the RMS peak occurrences are higher than 40% are considered, disregarding as low priority points the cases corresponding to a low number of occurrences. The actual speed of the whole considered lengths remains within the range 280-310 km/h. Figure 12 highlights the correspondence between the detected contact force peaks and the RMS peaks of the summed acceleration signals. It is not always possible to find one-to-one correspondence between contact force peaks and RMS peaks, but, by considering the entire number of test runs available, the majority of defective points can be identified. In Figure 12a, the number of contact force occurrences higher than the TSI limit of 350 N is shown by vertical bars, and the number of RMS occurrences higher than the threshold of 70 m/s^2 (with reference to the sum of leading and trailing collector accelerations) is indicated by circular markers. Nine out of thirteen force peaks recurring in more than 40% of runs (i.e. 3 out of 7 runs) are identified by RMS peaks recurring at least in 40% of runs. Three out of thirteen force peaks recurring in more than 40% are identified by RMS peaks recurring in less than 40% of runs. At only one position, km 61.8, the contact force peaks do not correspond to a RMS exceeding the selected threshold (70 m/s^2). Moreover, the method does not give false alarms but demonstrates good reliability: in only two occurrences (km 69.8, km 73.2) the RMS threshold is exceeded without the contact force threshold being exceeded. It is in any case remarkable that in the last case contact force values close to 300 N are found.

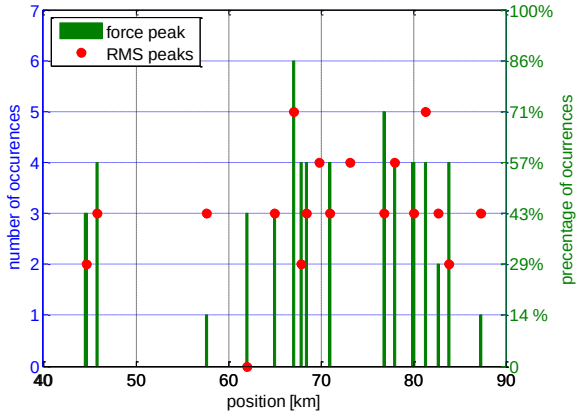

(a)

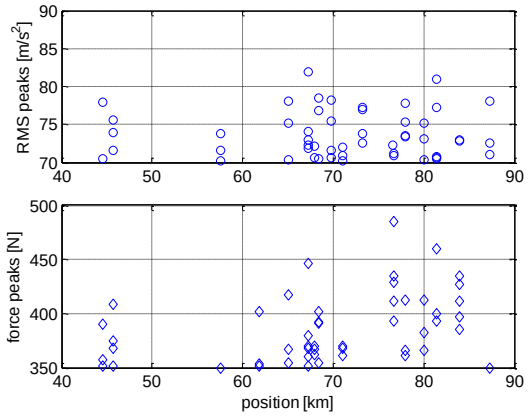

(b)

Figure 12: Comparison of the detected contact force peaks to the acceleration RMS peaks.

The 70 m/s^2 RMS threshold was chosen based on a preliminary statistical analysis of contact force and RMS peaks, showing that it is the most recurrent RMS values corresponding to the force limit of 350 N. The effect of choosing a threshold level higher than 70 m/s is the decrease of the hot-spots detected, the effect of choosing a lower threshold is the increase of the alarms given by the RMS algorithm non corresponding to any force peaks detected. Depending on the

dynamic interaction of the pantograph-catenary couple, the threshold value is likely to change when a different system is taken into account: in these cases an experimental data base must therefore be compiled before applying the proposed diagnostic algorithm.
Figure 12b shows the RMS values (top) and contact force peak values (bottom). The spread of contact force peaks at each location varies from 60N to 100 N, being wider than RMS spread. Considering that contact force and accelerations have different frequency ranges (20 Hz and 250 Hz respectively), although a correspondence of contact force and acceleration RMS peaks was found, it was not possible to find a clear correspondence between the intensity of contact force peaks and the corresponding acceleration RMS values.

5. DETECTION OF OVERHEAD LINE DISTRIBUTED DEFECTS

Defects such as incorrect conductor mechanical tension, stagger arm misregulation or incorrect dropper location generate an alteration of contact wire height, which results in distributed contact wire irregularity. This irregularity is a source of excitation for pantograph and collectors, so that high contact wire irregularity corresponds to an increase in the overall acceleration levels on both front and rear collectors. In order to use collector acceleration strength to identify the catenary lengths with high contact wire irregularity, the same kind of analysis performed in paragraph 4 for the detection of local defects can be used (i.e. RMS value of both collector accelerations computed over a time window with proper overlap). Since distributed contact wire height irregularity presents wave lengths higher than a span length [12], a larger window length can be adopted for this analysis, corresponding for example to 300 m (T=3.6 s for 300 km/h speed). At the same time a lower overlap is needed, since the phenomenon to be detected has a longer duration, and lower precision is required in position identification. The RMS can be effectively computed in real time either by using the time-samples, as in the case of the algorithm for local defect detection in section 4, or based on the results of a Fast Fourier Transform (FFT). As for the latter case, the leakage error due to the use of rectangular window does not affect the outcome of the defect identification, and this window is therefore preferred in order to keep as low as possible the number of operations required in the real time algorithm. Figure 13 shows the RMS of experimental accelerations (frequency content 0.5-250 Hz) computed with a mobile time window T=3.6 s and overlap 66% . Along 70 km of track covered, three points exceed the set limit, at km 68, km 45.5 and km 13, indicating an increase in acceleration intensity, and therefore a decrease in current collection quality. Moreover, as mentioned above, it can be seen that the acceleration level on the front collector (Figure 13a) is higher than that on the rear collector (Figure 13b), because the front collector interacts first with droppers and singular points.

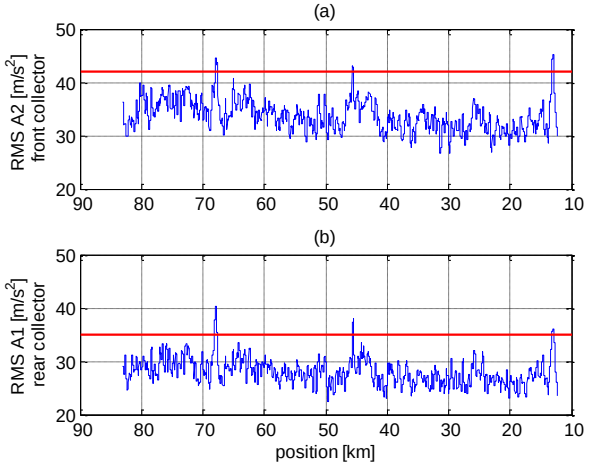

Figure 13: Acceleration RMS values computed over 70 km, with the mobile time window T=3.6 s, overlap 66%. Frequency content 0.5-250 Hz (a) Front collector. (b) Rear collector.

An irregularity in contact wire height, which generates an anomaly in pantograph trajectory, can be discovered for all of the three detected positions by using the pantograph standard measurement set-up as reference. Figure 14 shows, in an enlarged view over 1.5 km, contact strips trajectory (a), frame displacement (b) and stagger (c) corresponding to the peak at km 68 of the mobile RMS in Figure 13. An overhead line length placed at a different height is clearly visible from km 68 to km 67.5. This section represents an entire contact wire regulation, as detectable by the stagger in Figure 14c. Moreover, both contact strip trajectory and frame motion are evidence for a higher motion amplitude at span frequency along the defective section, which indicates a change in pantograph-catenary interaction. Table 2 shows the contact force mean values and the standard deviations measured both in the standard length and in the faulty length from km 68 to 67.5. The standard deviations of total, front and rear collector contact force are much higher in the faulty section.

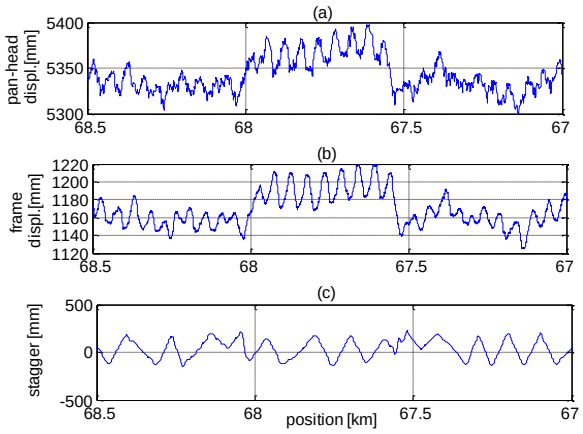

Figure 14: Standard set-up measures corresponding to a misplaced catenary length (km 68-67.5). (a) Pan-head trajectory. (b) Pantograph frame displacement. (c) Stagger.

	Standard catenary	Defective catenary (km 68-67.5)
Total	37.2	46.6 (+25%)
Front collector	22.9	27.4 (+20%)
Rear collector	20.2	26 (+29%)

Table 2: Contact force mean values and standard deviations: (a) Standard catenary length. (b) Defective catenary length (km 68 to km 67.5).

Figure 15 shows, in an enlarged view, contact strips trajectory, frame displacement and stagger corresponding to the peaks at km 45.5 (Figure 15a) and km 13 (Figure 15b) of the mobile RMS in Figure 13. Once again it can be seen that an irregularity in contact wire position is detected by the RMS analysis: in the former case (Figure 15a) a contact wire gradient is clearly visible from 45.8 to 45.3 in pan-head and articulated frame displacement; in the latter (Figure 15b) an irregularity in contact wire height is evident from km 13.2 to km 12.9.

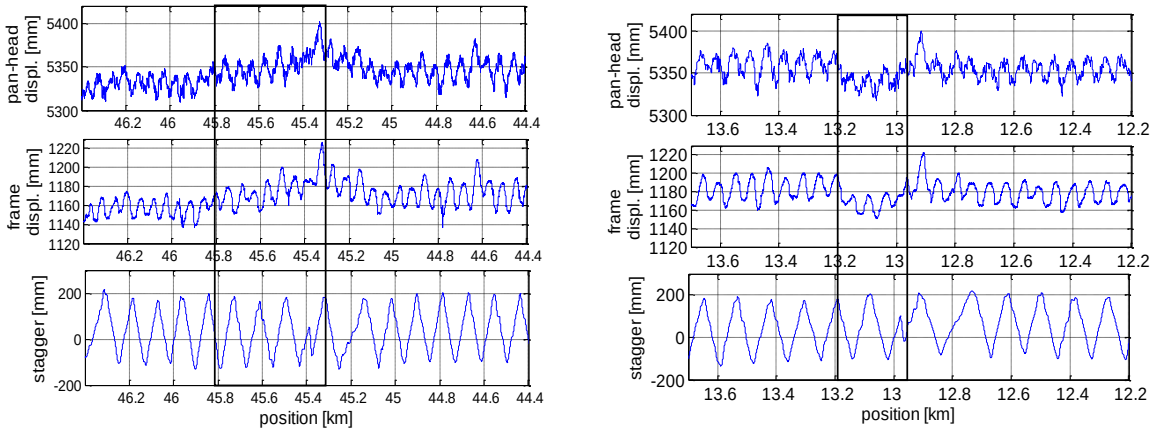

(a) (b)

Figure 15: Standard set-up measures corresponding to the catenary length (a) km 46.4-44.4, (b) km 13.7-12.2.

It is very important to underline that in the last two cases the standard deviations of the 0-20 Hz contact force measured in the lengths with irregular contact wire positioning do not show an increase with respect to the standard deviation computed in regular catenary lengths, as shown in Table 3.

	Standard catenary	Defective catenary (km 45.8-45.3)	Defective catenary (km 13.2-12.9)
Total [N]	37.2	32.7(-12%)	36.6(-2%)
Front [N]	22.9	21.1 (-8%)	23.1 (+1%)
Rear [N]	20.2	16.7 (-17%)	20.1 (-0.5%)

Table 3: Contact force standard deviations (0-20 Hz). Standard catenary length and defective catenary length.

This observation leads to the main conclusion that the extension of the measuring range over the classical 0-20 Hz band, and in particular up to the frequencies related to collector flexural modes, permits the detection of overhead line defects not identifiable solely by classical contact force measurements. This fact strengthens the argument advanced in [12], where the extension of the considered range up to the frequencies related to collector flexural modes is reported to be necessary for a more comprehensive assessment of current collection quality. To clarify this point Figure 16 shows the same RMS analysis as in Figure 13, now performed for different frequency bands of the acceleration signals: the same range 0.5-20 Hz as in contact force measurement, the range 55-160 Hz containing the first three collector modes, the overall range 0.5-250 Hz which is the same as in Figure 13. The RMS function obtained for the 55-160 Hz and 0.5-250 Hz ranges are very similar, whereas the 0.5-20 Hz RMS presents a different shape, with some peaks located at different track positions. Different information can therefore be obtained using different frequency ranges. If attention is focused on the three peaks at km 68, km 45.5 and km 13, it can be noted that, in agreement with the results of contact force standard deviations, in the case of the defect at km 68 a peak is detected by all the frequency range analyses, but the RMS computed on accelerations only in the 0.5-20 Hz frequency range is not able to detect the contact wire irregularities at km 45.5 and 13. In fact, in these cases, the 0.5-20 Hz RMS value does not differ that much from the average value.

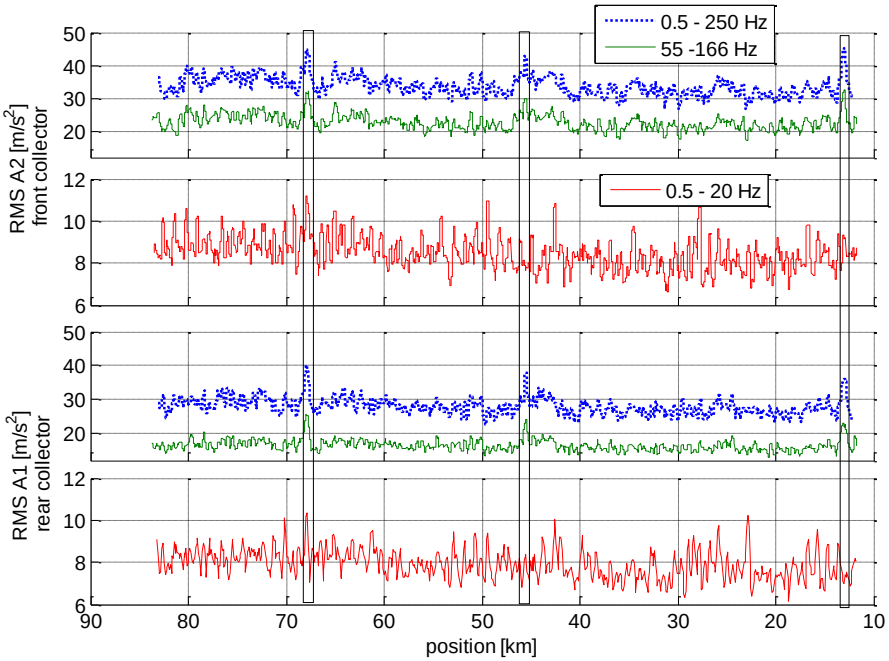

Figure 16: RMS values computed with a time window T=3.6 s, overlap 66% for different frequency ranges.

6. CONCLUDING REMARKS

A diagnostic system based on pantograph collector accelerations, using only two sensors, has been proposed and compared with a standard set-up for contact force measurement. Catenary local and distributed defects can be identified by RMS computed over mobile windows of different lengths. The results obtained showed good repeatability. The extension of the measuring range up to 200-250 Hz permits the detection of contact wire irregularities that cannot be identified considering only the 0-20 Hz frequency range.
The defects considered in this paper are mainly the result of construction imperfections. The introduction of other kinds of defect in the overhead line can be critical for safety and commercial reasons, nevertheless other types of defect can be analyzed both by numerical simulation and by HIL laboratory tests [16].

7. REFERENCES

[1] Foeillet G. - Coudert F. - Delcourt V. & al.: IRIS 320 is a global concept inspection vehicle,merging engineering and R&D tools for infrastructure maintenance. Proceedings of 8th World Congress on Railway Research (WCRR), Seoul, Korea, May 18-22, 2008.

[2] Ward C.P. – Weston P.F. – Stewart E.J.C – Li H. – Goodall R.M. – Roberts C. - Mei T.X. – Charles G. – Dixon R.: Condition monitoring opportunities using vehicle-based sensors, Proc. IMech, Part F: Journal of Rail and Rapid Transit, v 225, n 2, p 202-218, 2011.

[3] Kolbe M. - Baldauf W.: Compact contact force measurement system – online diagnosis of the overhead line system with regular trains, WCRR 2001, Köln, Germany, November 25-29, 2001.
[4] Kusumi S.- Fukutani T. - Nezu K.: Diagnosis of Overhead Contact Line based on Contact Force, Quarterly Report of RTRI, Vol. 47, No.1, February 2006.
[5] Collina A.- Fossati F.- Papi M.- Resta F.: Impact of overhead line irregularity on current collection and diagnostics based on the measurement of pantograph dynamics, Proc. IMech, Part F: Journal of Rail and Rapid Transit, v 221, n 4, p 547-559, 2007.
[6] Tanarro F. - Fuerte V.: OHMS - Real-time analysis of the pantograph-catenary interaction to reduce maintenance costs, 5th IET Conference on Railway Condition Monitoring and Non-Destructive Testing (RCM 2011), Derby, UK, 29-30 November 2011.
[7] Daadbin A. – Rosinski J.: Development, testing and implementation of the pantograph damage assessment system (PANDAS). WIT Transactions on the Built Environment, 114, p 573-578, 2010, Computers in Railways XII, COMPRAIL 2010.
[8] Bocciolone M. - Bucca G. - Collina A - Comolli L.: Pantograph-catenary monitoring by means of fibre Bragg grating sensors: results from tests in an underground line. Mechanical Systems and Signal Processing, v 41, n 1-2, p 226-238, December 2013.
[9] Schröder K. - Ecke W. - Kautz M. - Willett S. - Jenzer M. - Bosselmann T.: An approach to continuous on-site monitoring of contact forces in current collectors by a fiber optic sensing system. Optics and Lasers in Engineering, v 51, n 2, p 172-179, February 2013.
[10] Bocciolone M.F. - Bucca G. - Collina A - Comolli L.: An approach to monitor railway pantograph-catenary interaction with fiber optic sensors. Proceedings of SPIE - The International Society for Optical Engineering. 2010.
[11] Bruni S. – Carnevale M. – Facchinetti A.: Active control of the pantograph articulated frame to reduce contact force fluctuations in the low frequency range. Proceedings of the 13th mini Conference on Vehicle System Dynamics, Identification and Anomalies (VSDIA), Budapest, Hungary 5-7 November, 2012:
[12] Collina A. - Lo Conte A. - Carnevale M.: Effect of collector deformable modes in pantograph-catenary dynamic interaction. Proc IMech, Part F: J Rail Rapid Transit. v 223, n 1, p.1-14, 2009.
[13] Boffi P. - Cattaneo G. - Amoriello L. - Barberis A. - Bucca G. - Bocciolone M.F. - Collina A. - Martinelli M.: Optical fiber sensors to measure collector performance in the pantograph-catenary interaction. IEEE Sensors Journal, v 9, n 6, p 635-640, June 2009.
[14] A. Collina, S.Bruni: Numerical Simulation of Pantograph-Overhead Equipment Interaction, Vehicle System Dynamics, v 38, n 4, p 261-291, October 2002.
[15] Schröder K. - Ecke W. - Kautz M. - Willett S. - Unterwaditzer S. - Bosselmann T.- Rothhardt M.: Smart current collector - Fibre optic hit detection system for improved security on railway tracks. Measurement Science and Technology, v 24, n 11, November 2013.
[16] S. Bruni, A. Collina, A. Facchinetti: Pantograph and catenary condition based monitoring: theory and Hardware-in-the-Loop experiments. 12th MINI Conference on Vehicle System Dynamics, Identification and Anomalies (VSDIA 2010) Budapest, Hungary 8-10 November, 2010.

8. FUNDINGS

The Authors would like to gratefully acknowledge the “Joint Research Centre on Railway Transports” established by Fondazione Politecnico di Milano for providing financial support to this work.